Interactions of mRNAs and gRNAs involved in trypanosome mitochondrial RNA editing: structure probing of an mRNA bound to its cognate gRNA

S. S. Leung and D. J. Koslowsky

RNA 2001 7: 1803-1816

RNA (2001), *7*:1803–1816. Cambridge University Press. Printed in the USA.

DOI: 10.1017.S1355838201010305

Interactions of mRNAs and gRNAs involved in trypanosome mitochondrial RNA editing: Structure probing of an mRNA bound to its cognate gRNA

SHELDON S. LEUNG[1] and DONNA J. KOSLOWSKY[1,2]

[1]Interdepartmental Graduate Program in Genetics, Michigan State University, East Lansing, Michigan 48824, USA
[2]Department of Microbiology and Molecular Genetics, Michigan State University, East Lansing, Michigan 48824, USA

ABSTRACT

Posttranscriptional editing of trypanosome mitochondrial messenger RNA is directed by small guide RNAs (gRNAs). Using crosslinking techniques, we have previously shown that the gRNA base pairs to the mRNA via a 5′ anchor, whereas its 3′ U-tail interacts with upstream purine-rich mRNA sequences. The incorporation of crosslinking data into RNA folding programs produced similar structure predictions for all gRNA/mRNA pairs examined. This suggests that gRNA/mRNA pairs can form common secondary structure motifs that may be important for recognition by the editing complex. In this study, the structure of CYb mRNA crosslinked to gCYb-558 was examined using solution-probing techniques. The mRNA/gRNA crosslinked molecules are efficient substrates for gRNA-directed cleavage. In addition, when the cleavage assay is performed in the presence or absence of additional UTP, the activities of both the U-specific exonuclease and terminal uridylyl transferase (tutase) can be detected. These results indicate that a partial editing complex can assemble and function on these substrates suggesting that the crosslink captured the molecules in a biologically relevant interaction. The structure probing data directly show that the U-tail protects several mRNA bases predicted to be involved in the U-tail-mRNA duplex. In combination with our previous studies, these new data provide additional support for the predicted secondary structure of interacting gRNA/mRNA pairs.

Keywords: apocytochrome b; kinetoplasts; organelle gene expression; posttranscriptional processing; RNA–RNA interactions; RNA structure

INTRODUCTION

Mitochondrial RNA editing in *Trypanosoma brucei* is a unique phenomenon in which uridylates are precisely inserted or, less frequently, deleted from mRNA (Stuart et al., 1997; Hajduk & Sabitini, 1998; Estevez & Simpson, 1999). Over half of the mRNA transcript can be generated by U insertions, creating mRNAs twice as large as the gene that encodes them. Editing is essential, as this process is required to produce translatable transcripts. Short RNAs (50–70 nt), termed guide RNAs (gRNAs), contain the information for the sequence modifications. To direct these events, gRNAs must correctly pair with their cognate mRNAs. The annealing process requires hybridization of the 5′ anchor sequence of the gRNA to the complementary anchor binding site (ABS) located just downstream of the preedited domain. In addition to the anchor, gRNAs contain a guiding region of approximately 30–40 nt and a nonencoded 3′ uridine tail (U-tail; Blum & Simpson, 1990).

The current model for RNA editing invokes a cleavage-ligation mechanism (for review, see Stuart et al., 1997; Hajduk & Sabitini, 1998; Estevez & Simpson, 1999). The minimum number of enzymatic activities include a gRNA-directed endonuclease, terminal uridylyl transferase (tutase), 3′ U-specific exonuclease, and RNA ligase. These enzymatic "core" activities are found associated with other proteins in a large RNP complex termed the editosome (Pollard et al., 1992; Corell et al., 1996; Rusché et al., 1997; Panigrahi et al., 2001). The editosome must have the ability to assemble with hundreds of different gRNA/mRNA pairs. However, gRNAs and mRNAs do not contain common sequence elements that could be used for protein–RNA recognition. Instead, we hypothesize that interacting gRNAs and mRNAs form similar structural features that can assem-

Reprint requests to: Donna J. Koslowsky, Department of Microbiology and Molecular Genetics, Giltner Hall, Michigan State University, East Lansing, Michigan 48824, USA; e-mail: koslowsk@msu.edu.

ble with proteins into a core architecture essential to their function (Leung & Koslowsky, 1999). Using photoaffinity crosslinking, we have previously shown that three different gRNA/mRNA pairs can form similar structural elements. Each predicted fold contained three helices that flank the first few editing sites; a gRNA/mRNA anchor duplex, a U-tail/mRNA duplex, and a gRNA stem-loop similar to the one previously observed in the guiding region of gRNAs alone (Schmid et al., 1995).

We describe here additional support for these predicted structures, using chemical and enzymatic probing techniques. To overcome the technical difficulties associated with the solution probing of two interacting RNAs, we utilized a gRNA/mRNA pair that had been photochemically crosslinked at the 3′-most end (mRNA orientation) of their anchor duplex. A crosslink at this site would insure that the anchor duplex would be maintained during probing. In addition, because this crosslink is at the beginning of a known region of base-paired RNA, we anticipated it to be a minor constraint, limiting perturbation of the structure of the interacting RNAs. These crosslinked molecules support accurate gRNA directed endonuclease activity as well as tutase and exonuclease activity, strongly suggesting that they are recognized by the editosome. The structure probing data obtained directly show that the U-tail protects several mRNA bases predicted to be involved in the U-tail mRNA duplex. In combination with our previous crosslinking studies, these new data provide additional support for the predicted secondary structure of interacting gRNA/mRNA pairs (Leung & Koslowsky, 1999, 2001).

RESULTS AND DISCUSSION

Utilization of crosslinked RNAs for solution structure probing

In the current study, we focused on the interaction of 5′CYbUT with its cognate gRNA, gCYb-558. 5′CYbUT encompasses 88 nt of the 5′ end of preedited cytochrome *b*. Editing in this mRNA is developmentally regulated with edited message produced only in the procyclic (insect) and stumpy bloodstream stages of the trypanosome life cycle (Feagin et al., 1987, 1988). gCYb-558 directs editing at the first seven editing sites, resulting in the addition of 21 Us (Fig. 1A; Riley et al., 1994). Earlier studies have established secondary structure models for the gRNA alone, the mRNA alone, and the mRNA interacting with its cognate gRNA (Piller et al., 1995; Schmid et al., 1995; Leung & Koslowsky, 1999, 2001). Schmid et al. (1995) elucidated the secondary structure of several gRNAs including gCYb-558. These molecules appear to fold into two consecutive hairpin elements. The 5′ end of the gRNA is in a single-stranded conformation followed by a small hairpin that contains the anchor sequence. The guiding region is contained within the second, much larger stem loop whereas the U-tail appears to have a single-stranded conformation. The 5′ end of preedited cytochrome *b* is predicted to form a highly ordered stem-loop structure with the first three editing sites localized within the terminal loop (Fig. 1B). Interestingly, the ABS is contained within the closing stem duplexed to part of the purine-rich sequence thought to be involved in U-tail interactions (Leung & Koslowsky, 1999, 2001). The proposed structure for the gRNA/mRNA interaction is based on photoaffinity mapping of the 5′ and 3′ ends of gCYb-558 along 5′CYbUT (Leung & Koslowsky, 1999, 2001). This predicted structure contains three elements: (1) a gRNA/mRNA anchor helix, (2) a U-tail/mRNA helix, and (3) a gRNA stem-loop (Fig. 1C). To provide additional evidence for this proposed structure, 5′CYbUT was crosslinked to gRNA with (gCYb-558) and without a U-tail (gCYb-558sU, sans U). These crosslinks were then 5′-end labeled (mRNA) and structure probed in parallel, allowing us to investigate the interactions of the U-tail with its cognate message. Ribonucleases T1 and T2 along with Mung Bean nuclease (MBN) were used to identify single-stranded sequences, and methidium-propyl-EDTA-iron(II) (MPE-Fe(II)) was used to probe double-stranded regions.

To generate crosslinked substrates, gRNAs were transcribed in the presence of guanosine 5′-monophosphorothioate (GMPS). The resulting thiol group at the 5′ end was then coupled to azidophenacyl bromide (APA) by nucleophilic displacement of bromine. APA-modified-gRNAs and mRNAs were annealed and exposed to 312 nm light as previously described (Leung & Koslowsky, 1999). UV treatment utilizing 5′-APA-modified gRNAs produces one mRNA dependent crosslink that has been mapped to the 3′ end (mRNA orientation) of the gRNA/mRNA anchor duplex. Therefore, these crosslinked RNAs maintain the anchor duplex, an element that readily forms and is required for the process of editing. Crosslinks were gel purified and the mRNAs in the crosslinks were 5′-end labeled using T4 kinase.

Single-strand-specific nucleases

RNase T1 was used to identify unpaired Gs, as T1 specifically cleaves 3′ of single-stranded G residues (Fig. 2; Ehresmann et al., 1987). T1 probing of mRNA alone revealed three Gs (G66, G67, and G68) that were very sensitive to cleavage (Fig. 2A). These Gs map to the terminal loop of the predicted structure of 5′CYbUT and flank the first two editing sites (see Fig. 1A,B). The sensitivity of the loop to T1 was in agreement with previous observations (Piller et al., 1995). The remainder of the cleavages in the mRNA were minor in comparison, suggesting that the stem-loop structure of 5′CYbUT is stable. Minor cleavages were observed in

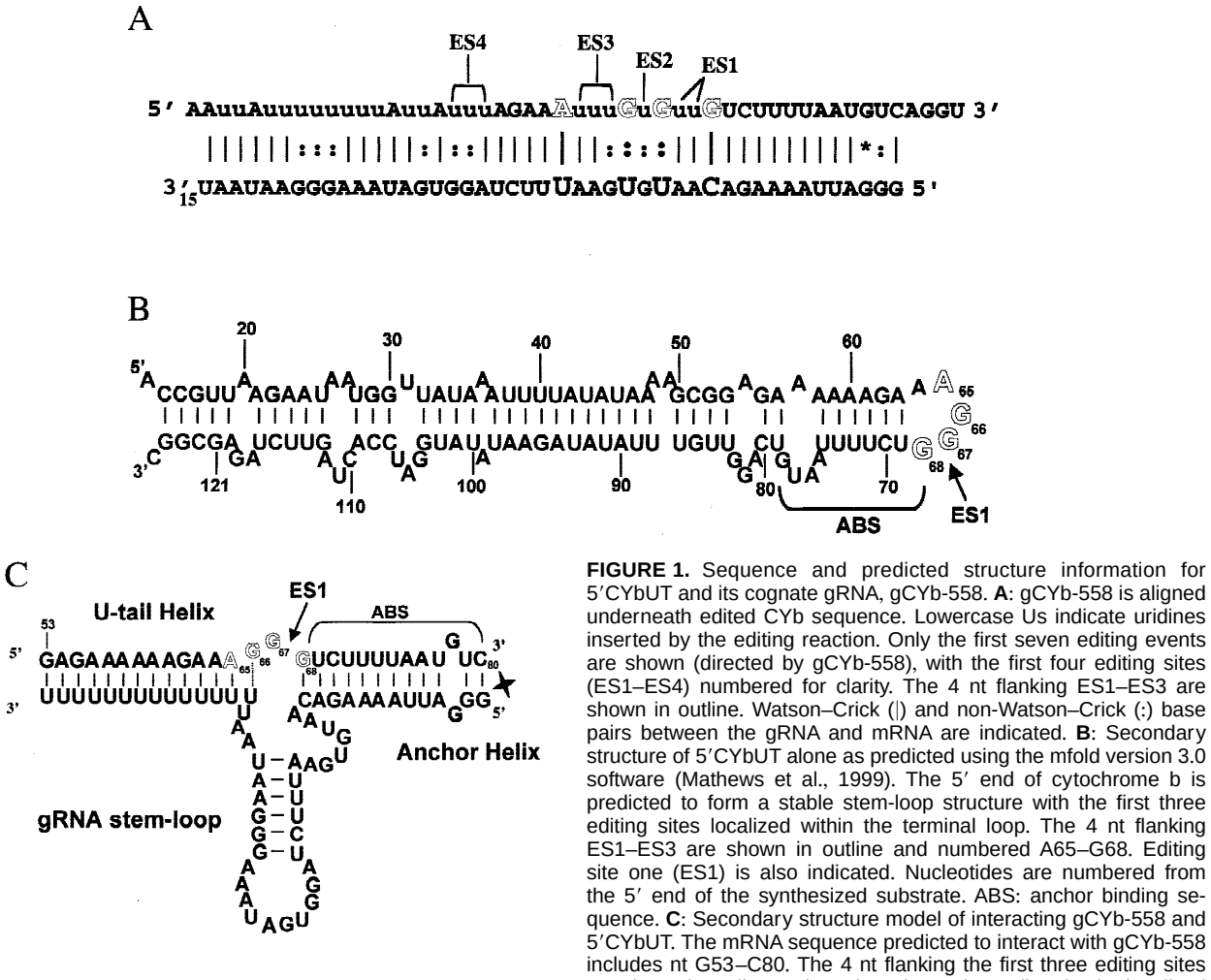

FIGURE 1. Sequence and predicted structure information for 5′CYbUT and its cognate gRNA, gCYb-558. **A**: gCYb-558 is aligned underneath edited CYb sequence. Lowercase Us indicate uridines inserted by the editing reaction. Only the first seven editing events are shown (directed by gCYb-558), with the first four editing sites (ES1–ES4) numbered for clarity. The 4 nt flanking ES1–ES3 are shown in outline. Watson–Crick (|) and non-Watson–Crick (:) base pairs between the gRNA and mRNA are indicated. **B**: Secondary structure of 5′CYbUT alone as predicted using the mfold version 3.0 software (Mathews et al., 1999). The 5′ end of cytochrome b is predicted to form a stable stem-loop structure with the first three editing sites localized within the terminal loop. The 4 nt flanking ES1–ES3 are shown in outline and numbered A65–G68. Editing site one (ES1) is also indicated. Nucleotides are numbered from the 5′ end of the synthesized substrate. ABS: anchor binding sequence. **C**: Secondary structure model of interacting gCYb-558 and 5′CYbUT. The mRNA sequence predicted to interact with gCYb-558 includes nt G53–C80. The 4 nt flanking the first three editing sites are shown in outline and numbered. ES1 is predicted to be localized to an internal bulge at the juncture of three helices, the anchor helix, the U-tail helix and the gRNA stem-loop. ABS: anchor binding sequence. Large star: position of the crosslink covalently linking the mRNA to the gRNA.

internal bulges and in short helices adjacent to internal bulges where one might expect some breathing and hence susceptibility to T1 cleavage. These included cleavages at G50, G52–53, G55, G62, G78, and G82–83.

Probing of gRNA-crosslinked RNA with T1 revealed that the presence of gCYb-558 significantly reduced the cleavage susceptibility of the three Gs previously found in the terminal loop of 5′CYbUT alone (Fig. 2B,C). Unexpectedly, the gRNAs presence did not appear to greatly affect cleavage at any site other than G78 (located 2 nt 5′ of the crosslink). Furthermore, no significant changes in sensitivity were observed in the presence or absence of the U-tail (gCYb-558 and gCYb-558sU, respectively). The U-tail is predicted to interact with a purine-rich sequence that we term the upstream U-tail stabilization element (uUtSE). This element covers bases G53 through G66 (Fig. 2B). We expected protection of at least the two internal Gs within this sequence in the presence of the U-tail/mRNA duplex. However, no significant difference in the reactivity of these Gs was observed using gCYb-558 or gCYb-558sU. Cleavages at G53 and G55 may be attributed to some flexibility in the U-tail interactions. Previous crosslinking studies indicated that the 3′ end of the U-tail could crosslink with a range of 4–5 nt (C51–G55). This flexibility may make it difficult to detect cleavage differences between the +U-tail/−U-tail substrates using RNase T1. Equal cleavage of G62 in the presence or absence of the U-tail is more difficult to understand. Cleavage of G62 was also often observed in the mRNA alone, even though it is predicted to be part of the terminal loop closing stem (Fig. 2A). In other experiments, however, some protection of this nucleotide was observed in the mRNA alone as compared to mRNA crosslinked to either gCYb-558 or gCYb-558sU (data not shown). This suggests that the G62–G66 nucleotides may not stably interact with the U-tail.

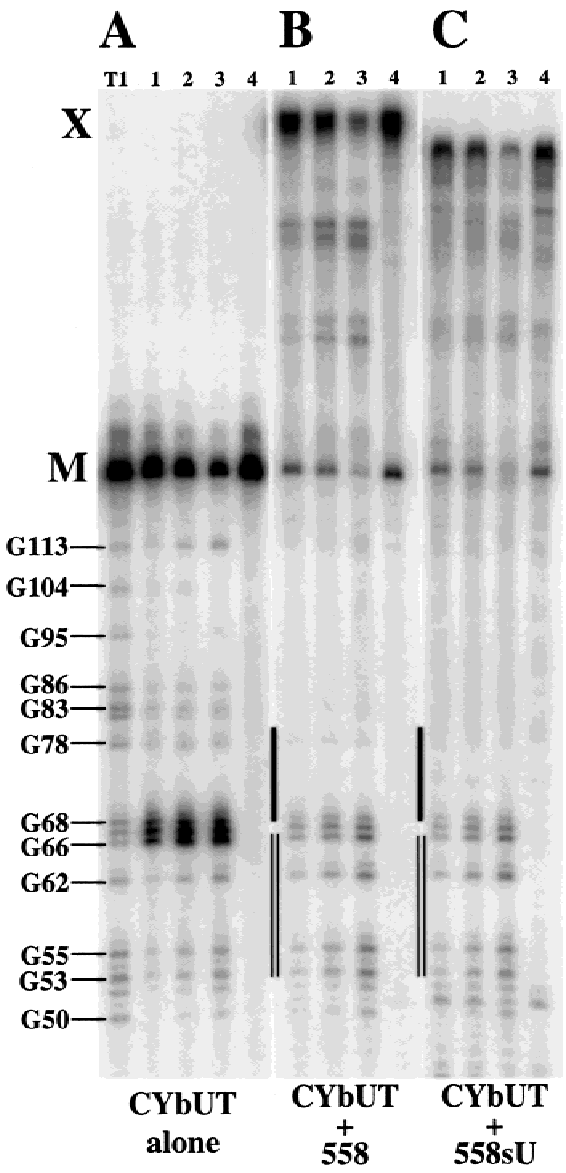

FIGURE 2. RNase T1 secondary structure analysis of 5′CYbUT (**A**) as compared to 5′CYbUT crosslinked to gCYb-558 (**B**) and to gCYb-558sU (no U-tail; **C**). Lanes 1–3: increasing amounts of T1 (0.025, 0.05, and 0.1 U). Lane 4: undigested RNA. T1: a T1 ladder generated under denaturing conditions. The solid line and double line denote the position of the anchor binding site (ABS) and predicted upstream U-tail sequence element (uUtSE), respectively. Specific G residues are indicated on the left. X and M indicate crosslink and mRNA, respectively. Full-length mRNAs present in **B** and **C** are due to crosslink breakage during handling. Cleavage products larger than full-length mRNA in **B** and **C** are due to nuclease action downstream (3′) of the crosslink (5′ end of gRNA crosslinked to C80). These cleavage products cannot be mapped, as the presence of the covalently linked gRNA slows their mobility unpredictably.

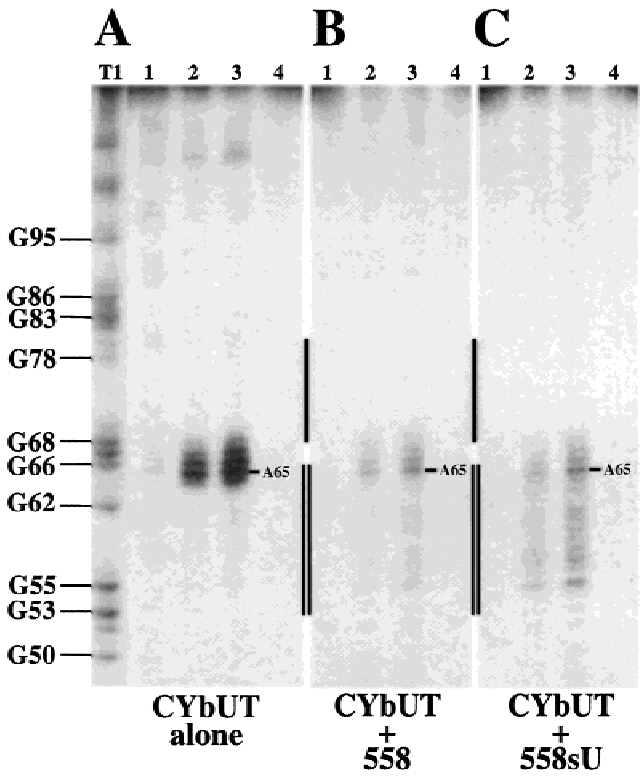

FIGURE 3. RNase T2 secondary structure analysis of 5′CYbUT (**A**) as compared to 5′CYbUT crosslinked to gCYb-558 (**B**) and to gCYb-558sU (**C**). Lanes 1–3: increasing amounts of T2 (0.0002, 0.002, and 0.04 U). Untreated RNA is shown in lane 4. T1, solid line, and double line are as described in Figure 2. Selected nucleotides of the ladder are indicated on the left. A65 is delineated in each panel for alignment purposes.

In contrast to RNase T1, the absence of the gRNA U_{15}-tail caused distinct differences in the pattern of cleavages obtained with two other single-strand-specific nucleases, RNase T2 and Mung Bean nuclease. RNase T2 cleaves single-stranded RNA 3′ of all four ribonucleotides with a strong preference for adenylic acid bonds (Uchider & Egami, 1967). T2 also highlighted the terminal loop of 5′CYbUT alone, showing a marked preference for A64–G67 (Fig. 3A). At high concentrations of T2, weak cleavage of G68 and A63 could be seen. The rest of 5′CYbUT was again remarkably resistant to T2.

A sharp reduction in cleavage in the region containing the initial editing sites was once again observed in the presence of crosslinked gRNA (Fig. 3B,C). Despite this inhibition, T2 did cleave in this region with distinct bands observed at A65 and G66. At higher T2 concentrations, weak cleavage of G67 was observed. However, the presence of a U-tail on the gRNA appeared to protect the A54–A64 region (Fig. 3B). Crosslinks lacking the U-tail showed increased T2 cleavage of the uUtSE region from A54 to A64. This indicated that the U-tail did protect the uUtSE, supporting the predicted structure.

The pattern of cleavage obtained with MBN was remarkably similar to that observed with RNase T2. Whereas this nuclease is described as having no nucleotide specificity (Kowalski et al., 1976), in our hands it also appeared to show a strong A bias. Within the mRNA alone, the most sensitive sites were again lim-

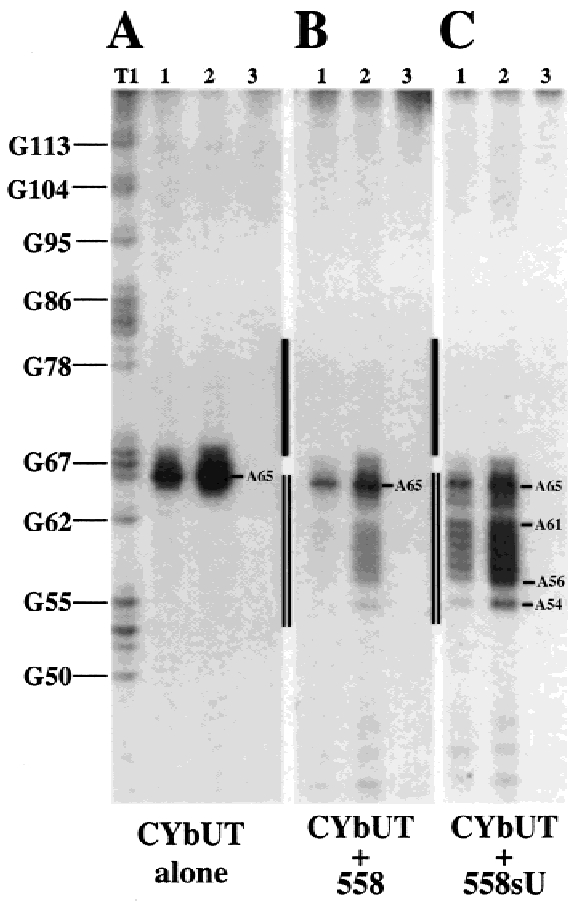

FIGURE 4. Mung Bean Nuclease secondary structure analysis of 5′CYbUT (**A**) as compared to 5′CYbUT crosslinked to gCYb-558 (**B**) and to gCYb-558sU (**C**). Increasing amounts of MBN (0.5, 1.0 U) were used (lanes 1–2). RNA not incubated with MBN is shown in lane 3 and the T1 ladder is labeled T1. Selected nucleotides of the ladder are shown on the left. Solid and double lines are as described in Figure 2.

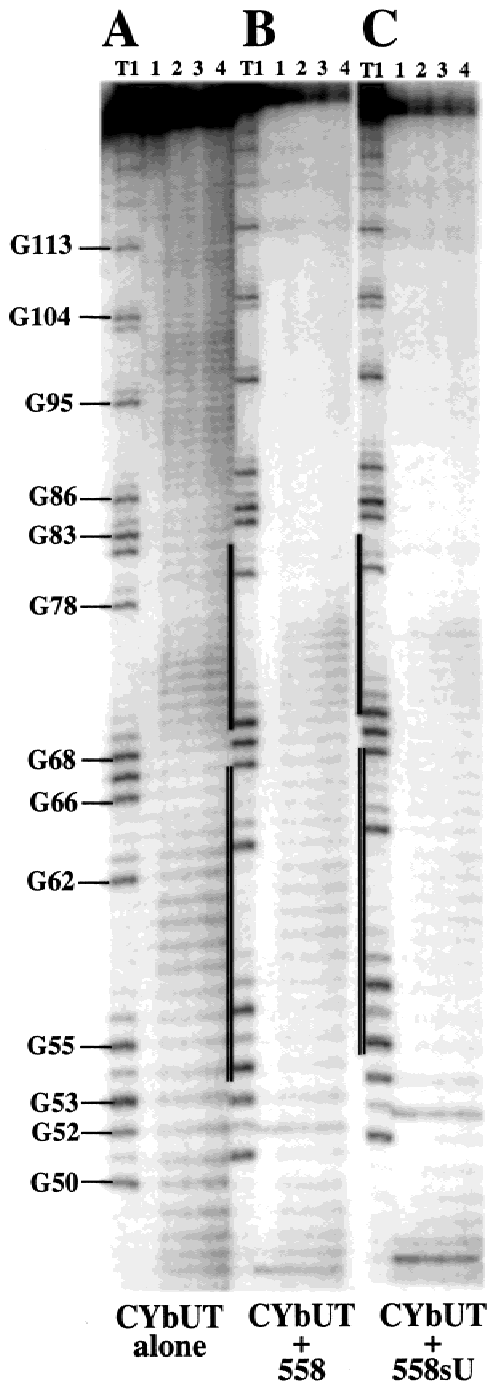

FIGURE 5. MPE-Fe (II) was used to probe double-stranded regions of 5′CYbUT alone (**A**), 5′CYbUT+gCYb-558 (**B**), and 5′CYbUT+gCYb-558sU (**C**). Aliquots were taken every 2 min (lanes 1–4 correspond to 0-, 2-, 4-, and 6-min incubations). T1 represents the ladder. Lines are as in Figure 2. Selected nucleotides of the ladder are shown on the right. Each reaction (**A**, **B**, and **C**) was loaded and electrophoresed into the gel before the next reaction, hence the offset in the bands.

ited to the terminal loop with the most prominent cleavages at A65 and G66, as previously observed (Piller et al., 1995; Fig. 4A). Less prominent, but distinct cleavages were also observed at A64 and G67. An increase in MBN concentration increased the intensity of the cleavages observed in this region, but did not otherwise change the cleavage pattern. Alignment with the T1 ladder is offset because MBN produces fragments with a 3′OH group as opposed to the 2′3′ cyclic phosphate generated by RNase T1 (Cruz-Reyes et al., 1998). In the presence of crosslinked gRNA, a distinct change in the cleavage pattern was observed (Fig. 4B,C). At the lowest concentration of MBN utilized, a single prominent cleavage at A65 was observed when the mRNA was crosslinked to gCYb-558 (+U-tail; Fig. 4B). Higher concentrations of MBN increased the number of cleavages observed with sensitive sites detected at A54, A56–A61, and A63–G67. In contrast, when crosslinked to gCYb-558sU (no U-tail), even the lowest concentration of nuclease cleaved nucleotides in the A54–G67 region (Fig. 4C). At the highest concentration utilized, the intensity of cleavage in this region approached that of A65 and G66, the most dominant cleavage sites. This correlates well with protection of the A54–A63 re-

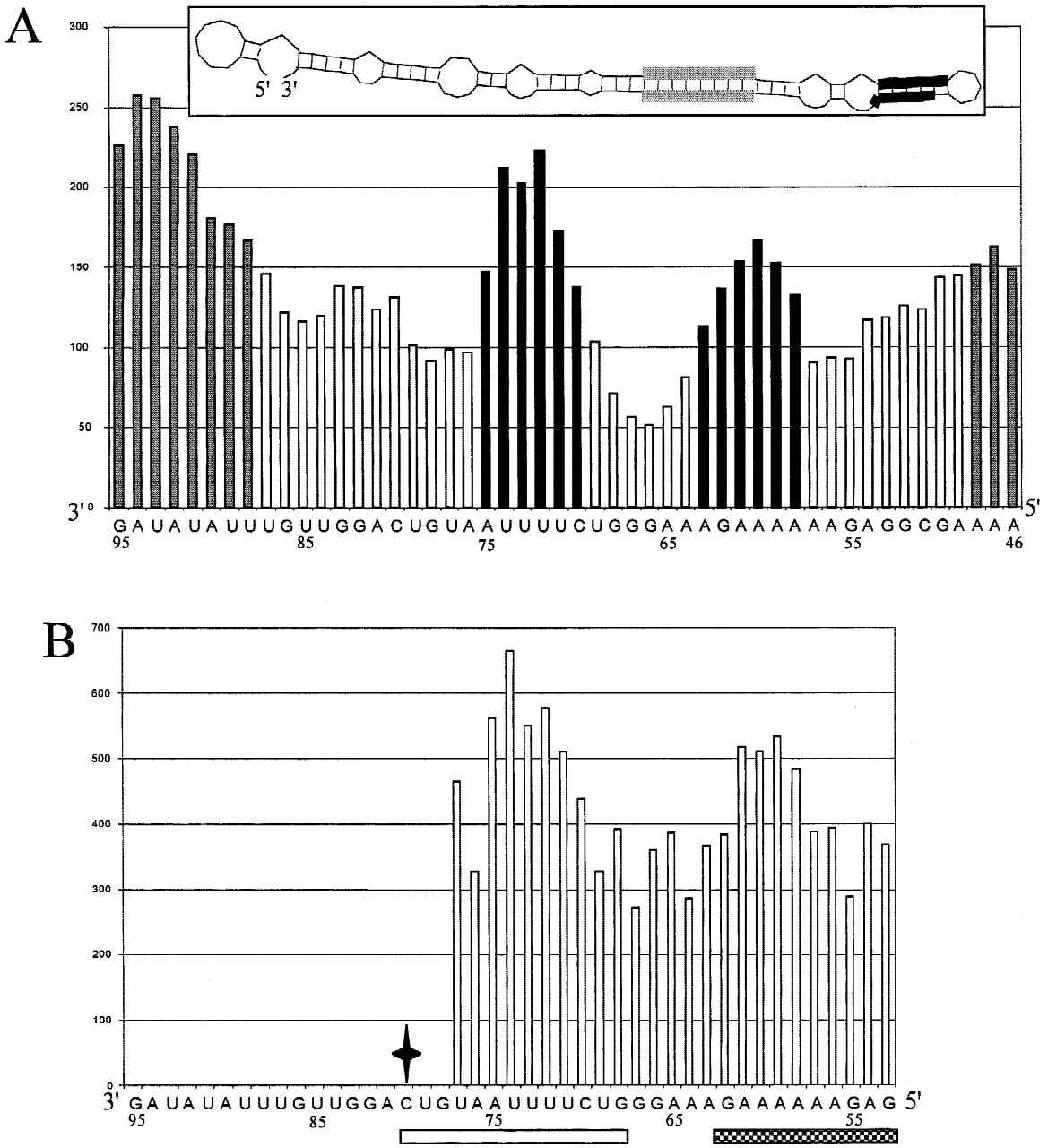

FIGURE 6. Quantitation of MPE-Fe(II) cleavage. **A**: Cleavage of 5′CYbUT alone was quantitated using a phosphorimager (lane 4 of Fig. 5A). The regions that show the highest sensitivity to MPE-Fe(II) are highlighted in black and dark gray. These regions correspond to two duplexes shown in the same colors in the predicted structure shown in the insert. Data from shorter run gels suggest the region at the right (A46-A48) extends farther upstream; hence the top dark gray line (insert) is longer than what is shown in the bar graph. **B**: Quantitation of 5′CYbUT+gCYb-558 cleavage (lane 4 of Fig. 5B). The sequence bound by the gRNA anchor (open box) and the uUtSE (checkered box) both show increased cleavage by MPE-Fe(II). Star above C80 indicates position of crosslink with gCYb-558. **C**: The uUtSE shows consistently higher MPE-Fe(II) cleavage in the presence (square) versus the absence (triangle) of the U-tail. Cleavage was normalized against the strongest cleavage observed in the anchor duplex. Data presented is the average of three experiments. (*Figure continues on facing page.*)

gion by the U-tail. These data support the secondary structure model, but indicate that the U-tail/mRNA duplex is not a stable interaction, allowing MBN to cleave the mRNA some of the time. With all three nucleases, no detectable differences in the cleavage patterns upstream of A54 were observed, indicating that the U-tail did not interact with regions farther upstream.

MPE-Fe(II)

Base-paired regions were examined using methidium-propyl-EDTA-iron(II), as RNase V1 is no longer commercially available. In the presence of O_2 and DTT, intercalated MPE-Fe(II) produces hydroxyl radicals that diffuse and cleave both strands of a helix (Hertzberg

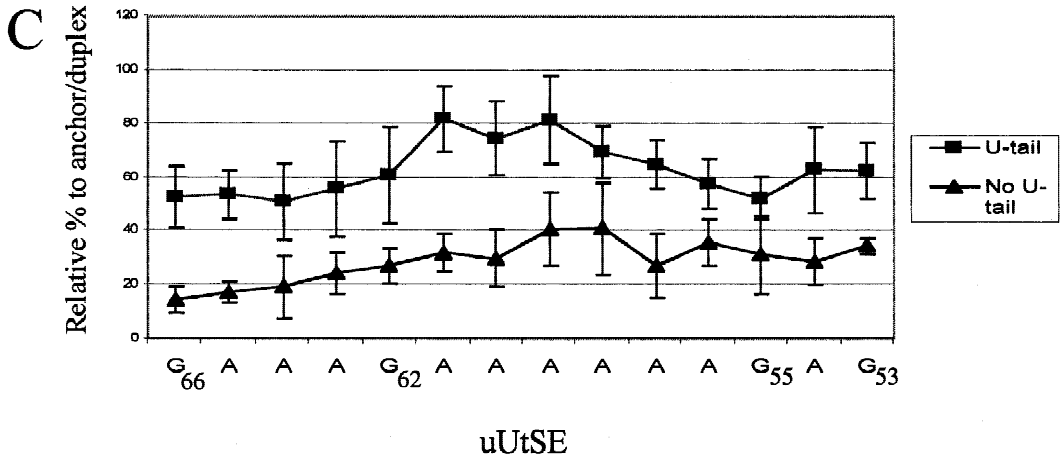

FIGURE 6. *Continued.*

& Dervan, 1984; Kean et al., 1985). Due to this diffusion, MPE-Fe(II) cleavage produces 3–5 cuts on both strands. Intercalation sites are identified by a peak of cuts (3–5 bases) on both strands, with helix geometry causing these cuts to be offset in the 3′ direction (Schultz & Dervan, 1983; Kean et al., 1985).

Probing of free 5′CYbUT with MPE-Fe(II) did not produce discrete sets of cuts, as virtually all the nucleotides examined were cleaved (Fig. 5A). However, it was clear that particular regions were much more sensitive to MPE-Fe(II) than others. Using a phosphorimager for quantitation, regions of increased sensitivity were mapped along 5′CYbUT alone, revealing that these regions corresponded to predicted sites of base-paired RNA. Figure 6A represents the quantitation of lane 4 in Figure 5A (6 min incubation). In this figure, the regions of increased sensitivity are paired (black and dark gray), indicating cleavage on both strands of a duplex (sites of MPE-Fe(II) intercalation). Gels run for a shorter time indicate that the region of sensitivity continues upstream of A46–A48 (data not shown). The MPE-Fe(II) data support two double-stranded regions, one just below the terminal loop (marked with a thick black line in the inset of Fig. 6A) and the other in the middle of the mRNA (dark gray line). The cleavages just below the terminal loop appear to be the result of a single intercalation site by MPE-Fe(II), producing a set of increased cleavages within a short region. The cleavages of the middle duplex were not confined to a short region, suggesting multiple intercalation sites, thus producing the broad shoulder of increased cuts (Fig. 6A and data not shown). The two regions of double-stranded RNAs identified by MPE-Fe(II) are in agreement with the predicted structure of mRNA alone.

Crosslinked RNAs showed two areas of increase MPE-Fe(II) cleavage, suggesting two regions of double-stranded RNA. In the presence of the gRNA, the anchor duplex (maintained by the crosslink) was highlighted by cleavage as expected (Fig. 5B,C). Figure 6B shows the quantitation of lane 4 of Figure 5B (5′CYbUT + gCYb-558). The nucleotides examined represent the sequence of interest: the anchor binding region and the uUtSE. Quantitation of cleavage 3′ of the crosslink (nt 80–95) was not possible, due to the presence of the covalently linked gRNA. Bases just 5′ of the crosslink (nucleotides 78–79; mRNA) did not produce a quantifiable signal, suggesting that the aryl group of the linkage might have sterically interfered with cleavage. The region surrounding ES1 was much less reactive, again emphasizing that the first few editing sites appear to be single-stranded in nature. To compare MPE-Fe(II) probing of the uUtSE in the presence or absence of the U-tail, the intensities of cleavages were normalized against the strongest cleavage site in the anchor/duplex. We assumed that MPE-Fe(II) reactivity within the anchor/duplexes in the presence or absence of the U-tail would be equal, as the sequences in this region are identical and the duplex is stabilized by the crosslink. The average of three experiments was used to compare the crosslinks. In the presence of the U-tail, cleavage within the uUtSE was strongest at A59, A60, and A61, with a reactivity approaching 80% of that seen in the anchor/duplex (Fig. 6C). Crosslinks produced with gCYb-558sU (no U-tail) showed consistently weaker cleavage in the uUtSE (Fig. 6C). These data are consistent with base pairing of the uUtSE only in the presence of the U-tail, as predicted.

Predicted structures

The data obtained from the nuclease and chemical probing experiments support the predicted structures for both the mRNA alone as well as the mRNA paired with its cognate gRNA (Table 1, Fig. 7A,B). 5′CYbUT alone folds into a stem-loop, making the terminal loop, which

TABLE 1. Summary of the chemical and enzyme accessibility data for 5′CYbUT.[a]

	5'CYbUT				CYbUT + 558				CYbUT + 558sU			
	T1	T2	MBN	MPE	T1	T2	MBN	MPE	T1	T2	MBN	MPE
G78	○											
U77								○○				○○
A76								○				○
A75				○○				●●				●●
U74				●●				●●				●●
U73				●●				●●				●●
U72				●●				●●				●●
U71				●●				●●				●●
C70				○○				○○				○○
U69								○				○
G68	●●	○			○				○			
G67	●●	●●	●●		○○	○	○		○○	○	○	
G66	●●	●●	●●		○○	○○	○○		○○	○○	○○	
A65		●●	●●			○○	●●			○○	●●	
A64		○○	●●				○			○○	○○	
A63				○○			○	○		○○	○○	
G62	○			○○	○			○	○			
A61				●●			○	●●		○○	○○	
A60				●●			○	●●		○○	○○	
A59				●●			○	●●		○○	○○	
A58				○○			○	●●		○○	○○	
A57							○	○		○○	○○	
A56							○	○		○○	○○	
G55	○				○				○			
A54							○			○	○	
G53	○				○				○			
G52	○				○				○			

[a]Relative reactivities are shown with ○, ○○, and ●● equivalent to marginally reactive to high reactivity. No quantitation of reactivity between the different nucleases or MPE is implied.

contains ES1–3, particularly accessible to single-strand specific nucleases. The stem of 5′CYbUT was particularly resistant to nuclease cleavage, suggesting that it is quite stable, whereas MPE-Fe(II) reactivity outlined two helices consistent with the predicted structure (Fig. 7A).

Crosslinking the gCYb-558 to 5′CYbUT clearly changed the structure of the mRNA. The intense cleavage at ES1 through ES3 in the terminal loop of the free mRNA was significantly reduced in the presence of crosslinked gRNA. The major decrease in reactivity is indicative of movement of these nucleotides from a terminal loop to a junction region that may be less accessible due to helical stacking interactions. In addition, probing of crosslinked 5′CYbUT provided direct evidence for the U-tail/mRNA duplex (Fig. 7B). Enhanced cleavage in the uUtSE (A54, A56–A61) by MBN and T2 in the absence of the U-tail contrasted with very weak cleavages in the presence of the U-tail (Table 1). This indicated that the U-tail base pairs with the uUtSE, providing protection to this sequence. The fact that cleavage is not completely abolished in the presence of the U-tail does suggest that this interaction is not very stable. However, the differential sensitivity to single-strand nucleases was very reproducible, giving consistent results upon multiple experimental runs. The presence of the U-tail also correlated with increased MPE-Fe(II) cleavage in the uUtSE, indicative of MPE-Fe(II) intercalation. The only modification to the predicted structure of the gRNA/mRNA pair suggested by the probing data involves the number of bulged nucleotides surrounding the first few editing sites. In our initial proposed structure, A64–G66 were part of the U-tail helix. It is clear from our analyses that these nucleotides are single stranded in the presence of the U-tail, suggesting that the bulged region at the juncture of the three helices involves 3 or 4 nt and the first three editing sites. In general however, the structure probing data from this study correlated well with our predicted secondary structure of gRNA/mRNA pairs. The biological significance of the RNA structure found upstream of the uUtSE is questionable as some vector sequence is included. For that reason, we did not present structure data obtained for this region.

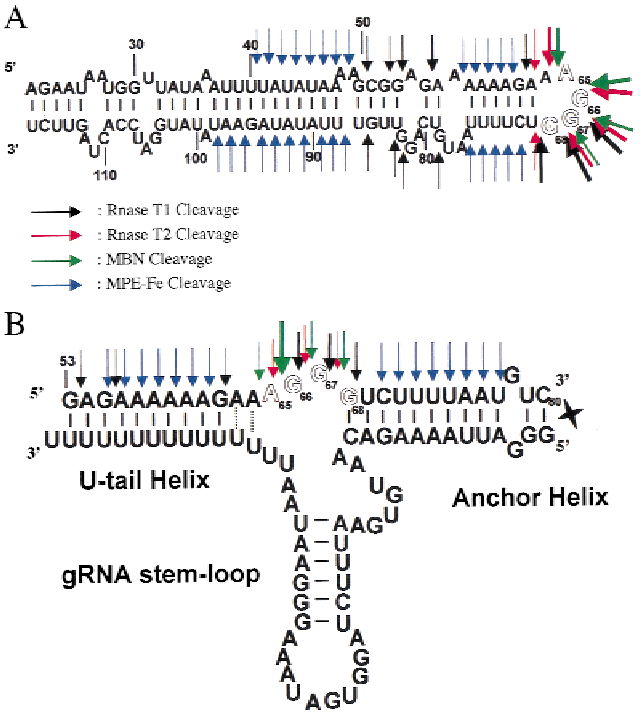

FIGURE 7. Summary of enzymatic and chemical probing of 5′CYbUT RNA alone (**A**) and crosslinked to gCYb-558 (**B**). Cleavages by T1 (black), T2 (red), MBN (green), and MPE-FeII (blue) are shown on the structures. Size of arrows indicate relative strength of cleavage observed.

Crosslinked substrates support editosome assembly

To determine if the crosslinked molecules formed structures that were biologically relevant, we examined whether they were substrates for the RNA editing machinery. Direct visualization of a full round of editing was not possible due to the branched structure of the crosslinked RNA. Therefore, we first looked to see if they would support the initial enzymatic activity in editing, gRNA-directed cleavage. To facilitate our analysis, four different 5′ crosslinks were examined, gCYb-558 with 5′CYbUT as well as gA6–14 with 3′A6UMT, A6PES1MT, and A6PES3MT. By utilizing multiple gRNA/mRNA pairs, we could examine cleavages directed at both U-insertion as well as U-deletion sites.

The CYb substrate, utilized in the structure probing, was described earlier. All A6 substrates are based on adenosine triphosphate synthase subunit 6 (91 nt of the 3′ end). A6 mRNA is edited throughout the life cycle and it is the paradigm system used for in vitro analysis of the editing reaction. Editing at the first 12 sites is guided by gA6–14 and includes both U insertions and U deletions (Bhat et al., 1990). To generate crosslinks using A6 substrates, the original A6 RNA was modified (M) so as to form a gRNA/mRNA duplex that included the 5′-most nucleotide of gA6–14 (3′A6UMT). These modified substrates efficiently produced crosslinked molecules with the 5′ end of gA6–14 correctly linked to the 3′ end of the ABS (data not shown). Partially edited A6 substrates were generated by PCR mutagenesis using 3′A6UMT as a template. A6PES1MT and A6PES3MT are identical to 3′A6UMT except that editing site 1 (ES1) and the first three editing sites (ES3) are fully edited, respectively (Fig. 8). Inclusion of the A6 substrates with 5′CYbUT gave us two substrates directed to cleave at a U-insertion site (5′CYbUT and A6PES1MT) and two substrates directed to cleave at a U-deletion site (3′A6UMT and A6PES3MT).

When incubated in editing active mitochondrial fractions, all four crosslinks supported accurate gRNA-directed endonuclease cleavage (Figs. 9 and 10). Crosslinked 3′A6UMT yielded a 5′ cleavage product that is 95 nt in length as expected for cleavage at ES1 (where two Us are deleted). However, an additional product, approximately 2 nt smaller, was also observed (Fig. 9A). Cleavage at ES2 (A6PES1MT, U-insertion site) produced only a single 5′ product of 92 nt, whereas cleavage at ES4 (A6PES3MT, U-deletion site) again produced a doublet of 5′ products (Fig. 9B,C). For all three A6 mRNAs, cleavage of the X-linked substrates was as efficient as that observed for the free mRNA controls (see Fig. 9A,B,C, lanes 4 and 5). Cleavage of substrates whose immediate editing sites require deletion events resulted in the generation of two products (3′A6UMT and A6PES3MT, Fig. 9A,C). Heterogeneous 5′ cleavage fragments have been previously observed at sites of deletion and are attributed to U-specific exonuclease activity (Cruz-Reyes & Sollner-Webb, 1996). In contrast, cleavage of both A6PES1MT and CYbUT (cleavage directed at U-insertion sites) resulted in a single cleavage product (Figs. 9B and 10A,B). We hypothesized that a single product was observed due to the lack of UTP required for the tutase activity. To test this hypothesis, we assayed the cleavage of the CYbUT crosslinked substrate in the presence of UTP (Fig. 10C). When UTP was added, an additional 5′ fragment 1 nt larger was observed for crosslinked 5′CYbUT. This implied that a single U had been added to the 3′ end of the 5′ fragment via tutase. Whereas the gRNA for 5′CYbUT directs the insertion of two Us at the site in question, the addition of only one U was observed. We suspect that the addition of two Us preferentially targets this 5′ product for religation as previously reported, making it difficult to detect (Kable et al., 1996; Igo et al., 2000). This would also explain why the addition of UTP caused a decrease in the amount of 5′ cleavage product observed. Ligase activity was present in our reactions as shown by the band above the free mRNA (marked “L”; Figs. 9 and 10). Periodate treatment of the mRNA blocks formation of this slower mobility product, suggesting that it is circularized mRNA (data not shown).

Isolation and handling of crosslinks resulted in the breakage of a fraction of the conjugate species, releas-

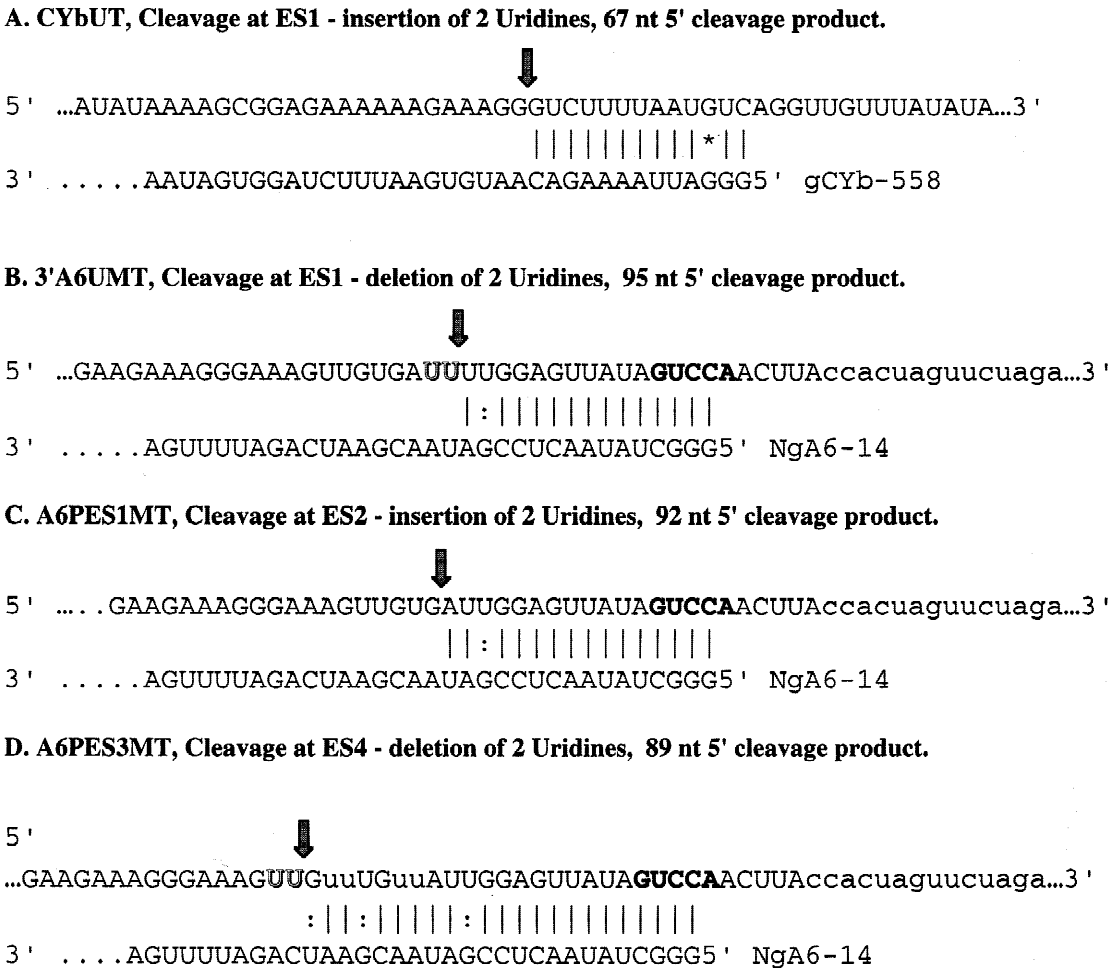

FIGURE 8. mRNA/gRNA crosslinked pairs used in the cleavage assays. **A**: 5′CYbUT + gCYb-558. **B**: 3′A6UMT + gA6-14. **C**: A6PES1MT + gA6-14. **D**: A6PES3MT + gA6-14. Only the sequences of interest are shown. gRNAs are aligned underneath their respective mRNAs. The modified sequence of the A6 substrates is shown in bold. Shadowed Us are deleted during editing, and arrows highlight the expected site of gRNA-directed endonuclease cleavage. Watson–Crick (|) and G:U base pairing (:) are indicated.

ing the free mRNA visible in our reactions (Wower et al., 1989; Burgin & Pace, 1990). We were concerned that the cleavage products observed could be generated by cleavage of the released free mRNA. Breakage of the mRNA/gRNA crosslinks would release the two RNAs in equal molar amounts. In the in vitro cleavage assays described to date, the generation of cleavage product requires the addition of excess gRNA in order to drive the reaction (Byrne et al., 1996; Kable et al., 1996; Seiwert et al., 1996). gRNA-directed cleavage of free mRNA utilizing a 1:1 mRNA:gRNA ratio is very inefficient (Fig. 9A,B,C, lanes 4, and Fig. 10A, lane 1). Efficient cleavage is only observed when the gRNA is supplied in excess (Fig. 9A,B,C, lanes 5, and Fig. 10A, lanes 2 and 3). In contrast, crosslinked substrates support efficient cleavage in the absence of exogenous gRNAs (Fig. 9A,B,C, lanes 1, and Fig. 10B, lane 2). Furthermore, the addition of excess gRNA did not increase cleavage of crosslinked mRNAs (Fig. 9A,B,C, lane 2).

These data indicate that the crosslinked mRNA/gRNA pairs are substrates that support accurate cleavage, terminal uridylyl transferase and exonuclease activities. These activities are complexed together in the editosome, suggesting that the crosslinked substrates are recognized by the editosome and allow for the assembly of an active complex. Thus, these crosslinked substrates have been captured in a biologically active state and they are appropriate substrates for structure probing studies.

CONCLUSIONS

The process by which active editosomes assemble onto gRNA/mRNA complexes is still unknown. Both gRNAs and mRNAs alone are able to support formation of RNP complexes that may represent specific steps in the assembly process (Göringer et al., 1994; Read et al., 1994; Koslowsky et al., 1996). However, we know that editing requires the interaction of both RNAs, arguing

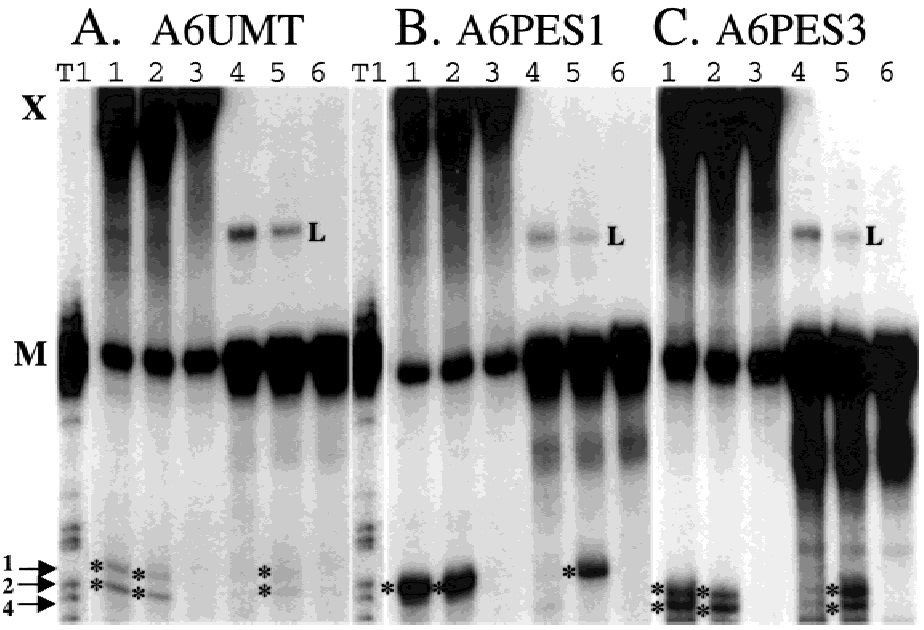

FIGURE 9. gRNA-directed cleavage of A6 substrates crosslinked to gA6-14. **A**: 3′A6UMT. **B**: 3′A6PES1MT. **C**: 3′A6PES3MT. Lanes 1–3: crosslinked substrates. Lanes 4–6: free mRNA and gRNA. Free mRNA present in the X-link lanes is due to the breakage of the linkage during handling. All lanes contained mt lysate except lanes 3 and 6. Lane 4: 1:1 gRNA:mRNA ratio. Lanes, 2, 5, and 6: 10:1 gRNA:mRNA ratio. T1: RNase T1 digest of denatured 5′-end labeled 3′A6UMT. T1 lane was scanned from a longer exposure of the same gel and duplicated for alignment purposes. The expected cleavage sites for ES1, ES2, and ES4 are indicated by numbered arrows. The editing cleavage products migrate out of phase with the RNase T1 ladder as RNase T1 generates 2′3′ cyclic GMP ends. The gRNA-directed cleavage products are highlighted by asterisks. The crosslink, free mRNA, and ligase-induced circular mRNAs are indicated by X, M, and L, respectively.

that final editosome assembly requires specific aspects of this interaction. Our previous crosslinking study mapped the position of the 5′ and 3′ ends of gRNAs along their cognate mRNAs. These data led to a predicted common structure for interacting gRNA/mRNA pairs involving a gRNA/mRNA anchor duplex, an upstream U-tail/mRNA duplex and a gRNA stem-loop. This suggests that structural aspects of the gRNA/mRNA interaction could play a role in editosome assembly and function. To provide additional evidence in support of our predicted structures, we solution probed 5′CYbUT crosslinked to gCYb-558. We chose to crosslink the two RNAs together, as probing of two interacting free RNAs introduces several technical problems.

5′ crosslinked molecules are substrates for activities connected with editing. Accurate cleavage of all crosslinked substrates was observed at the appropriate editing site, demonstrating that the RNAs supported gRNA-directed endoribonuclease activity. Furthermore, the UTP-dependent addition of a nucleotide to the 5′ cleavage product of crosslinked 5′CYbUT was indicative of tutase activity, whereas at sites of U deletion, U-specific exonuclease activity on 5′ cleavage products was observed. These enzymatic activities have been shown to associate together in a complex using glycerol gradient fractionation and chromatography (Pollard et al., 1992; Corell et al., 1996; Rusché et al., 1997). This argues that the editing complex interacts and assembles correctly on the crosslinked RNAs and that structures determined utilizing these molecules are biologically relevant.

The additional evidence presented for the U-tail/mRNA duplex supports the U-tail's role as a tether to hold the 5′ cleavage mRNA product during editing. The fact that this interaction is not very stable is also in agreement with experiments demonstrating that modified gRNA sequences with increased base pairing with the uUtSE function as better tethers (Seiwert et al., 1996; Burgess et al., 1999; Kapushoc & Simpson, 1999). Despite being presented with the full range of available upstream purines, the U-tail base pairs to mRNA sequences just upstream of the initial editing sites. The formation of two helices that flank the first few initial editing sites raises the possibility that these two helices function in concert to correctly present the initial editing sites to the editing complex. Alternatively, it may be that multiple helices surrounding the editing site are important for tertiary interactions that help stabilize the gRNA/mRNA interactions.

The results of this study indicate that 5′ crosslinked RNAs are ideal substrates to pursue the structural aspects of gRNA/mRNA interactions that could play a role in full editosome assembly, stability, and editing site presentation.

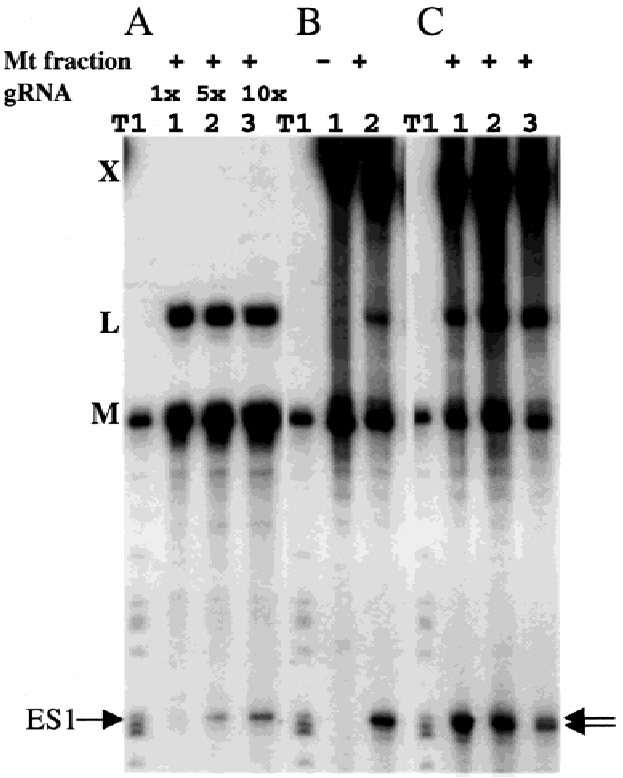

FIGURE 10. Cleavage of 5′CYbUT. **A**: Free 5′CYbUT and gCYb-558. Lanes 1–3: 1:1, 5:1, and 10:1 gRNA:mRNA ratio in the presence of mt lysate. **B**: Crosslinked 5′CYbUT and gCYb-558. Lane 1: no lysate control. Lane 2: crosslinked RNA in the presence of mt lysate. **C**: Lanes 1–3: crosslinked RNA in the presence of mt lysate and increasing concentrations of UTP (0, 0.1, and 0.25, respectively). The two products observed in the presence of UTP are highlighted by the double arrow. T1: T1-generated ladder. The expected cleavage site at ES1 is marked. The crosslink and mRNA are indicated by X and M, respectively. L indicates migration of circular mRNAs generated by the presence of precharged ligase in the active fractions.

MATERIALS AND METHODS

Oligodeoxynucleotides

A6 MOD Anchor: 5′-GGCCGCTCTAGAACTAGTGGTAA GTGGACTATAACTCC-3′, 38 nt;

A6PES1: 5′-CTTATTCTATAACTCCAATCACAAC TTTCCCTTTC-3′, 35 nt;

A6PES3: 5′-CTTATTCTATAACTCCAATAACAAA CAACTTTCCCTTTC-3′, 39 nt;

NgA6-14: 5′-AAAAAAAAAAAAAAATAATTATCAT ATCACTGTCAAAATCTGATTCGTT ATCGGAGTTATAGCCCTATAGTGA GTCGTATTAAATT-3′, 86 nt.

Transcription templates

5′CYbUT has been described before (Koslowsky et al., 1996). The A6 partially edited mRNA substrates were created from 3′A6UT using PCR with oligonucleotides T7 and 3′A6PES1 or 3′A6PES3 followed by a second round of amplification using T7 and A6 MOD Anchor (Koslowsky et al., 1996). mRNA templates were PCR amplified prior to use (Leung & Koslowsky, 1999).

Transcription

To facilitate 5′-end labeling, mRNAs were transcribed in the presence of 5 mM guanosine. The lack of phosphates in the nucleoside limits guanosine incorporation to the 5′ end while making it an efficient substrate for kinase end labeling. mRNA transcription reactions also contained 200 U of T7 RNA polymerase, 40 mM Tris, pH 8.0, 25 mM $MgCl_2$, 5 mM DTT, 2 mM spermidine, 0.01% Triton X-100, 16 U RNAsin, 1 U yeast pyrophosphatase, 1 mM GTP, and the remaining rNTPs at 2 mM. gRNAs were synthesized using the appropriate oligodeoxynucleotide (NgA6-14, NgCYb-558, and NgCYb-558sU) and the T7 oligonucleotide via the Uhlenbeck single-stranded T7 transcription method (Milligan et al., 1987). The T7 and NgCYb-558sU oligonucleotides have been previously described (Leung & Koslowsky, 2001). NgCYb-558 is identical to the NgCYb-558sU oligonucleotide except for the presence of 15 A residues on the 5′ end. Guanosine 5′-thiophosphate-containing gRNAs were transcribed in the presence of 7 mM GMPS and 1 mM rNTPs. mRNAs and gRNAs were gel purified on 6% and 8% denaturing polyacrylamide gels, respectively. RNAs were passively eluted from gels in 10 mM Tris, pH 7.8, 0.1% SDS, 2 mM EDTA, and 0.3 M NaOAc, pH 7.0, and recovered by precipitation.

Crosslinking

Modifications to the gRNAs and crosslinking conditions have been described previously (Leung & Koslowsky, 1999). RNAs were annealed using 2 to 5 molar amounts of mRNA to modified gRNA. Crosslinked RNAs were purified on 6% denaturing gels and recovered as described above.

End labeling

Up to 5 pmol of free or crosslinked mRNA were 5′-end labeled using 50 μCi of α^{32}P-ATP, 10 U of Kinase (New England Biolabs) and 1$\times$ Kinase buffer for 1 h at 37 °C. Unincorporated α^{32}P-ATP was removed by gel purifying the RNAs on a 6% denaturing gel.

Structure probing

Single-strand-specific probes

All reactions contained 30,000 cpm of 5′-end-labeled substrate and 5 μg of yeast tRNA. Substrates were denatured at 60 °C for 2 min and cooled to 27 °C (optimal temperature for procyclic trypanosome growth) at a rate of 2 °C per min. After 20 min at 27 °C, the enzymatic or chemical probe was added. Reactions were incubated for 10 min at 27 °C and terminated by phenol extraction. Products were separated on 8% denaturing polyacrylamide gels. The reaction conditions for the individual probes are described below. RNase T1 (Roche) digestions were carried out in 10 mM Tris, pH 7.5, 50 mM KCl, and 1 mM $MgCl_2$. Probing conditions for RNase T2 (Sigma) were as follows: 10 mM Tris, pH 7, 50 mM KCl, and

1 mM $MgCl_2$. Mung Bean Nuclease (NEB) reactions contained 30 mM NaOAc, pH 7, 50 mM NaCl, 5% glycerol, and 0.1 mM $MgCl_2$. $ZnCl_2$ (1 mM) was added with the nuclease. Reducing the magnesium concentration from 1 mM $MgCl_2$ to 0.1 mM $MgCl_2$ only increased the intensities of cleavages observed and did not change the overall pattern obtained (data not shown). Only data from probing reactions that resulted in significantly less than 50% cleavage of the input RNAs were used for interpretation as suggested by Christiansen et al. (1990). Cleavage analyses were based on a minimum of three different experimental runs for each nuclease. RNase T1 ladders were generated by incubating heat-denatured 5′-end-labeled mRNAs (~240,000 cpm) in 20 mM NaCitrate, 1 mM EDTA, and 2 U of RNase T1 for 10 min at 55 °C.

Probing with MPE-Fe(II)

MPE-Fe(II) (80 μM) was freshly prepared for each reaction from methidiumpropyl-EDTA (Sigma) and ferrous ammonium sulfate (Sigma; Vary & Vournakis, 1984; Kean et al., 1985). 5′-end-labeled RNA (200,000 cpm) and 8 μg of yeast tRNA were heated to 60 °C for 2 min and cooled to 27 °C at 2 °C/min in 10 mM Tris, pH 7.5, 50 mM KCl, and 1 mM $MgCl_2$. Before the addition of probe, a time zero aliquot was taken. MPE-Fe(II) was added to 20 μM followed by DTT to 6.25 mM. Aliquots were taken at 2-min intervals up to 6 min. Reactions were stopped with 10 M urea, 20 mM EDTA, 100 μg tRNA, 0.1% bromophenol blue, and 0.1% xylene cyanol. Aliquots were stored at −80 °C until separated on 12% denaturing polyacrylamide gels.

Structure prediction

Structures predictions were obtained using RNAstructure 3.5 and graphically displayed using RNAdraw version 1.1 as previously described (Matzura & Wennborg, 1996; Leung & Koslowsky, 1999; Mathews et al., 1999).

Cleavage reactions

Mitochondrial lysates were prepared from the procyclic stage of *Trypanosoma brucei brucei*, EATRO 1.7 and fractionated using glycerol gradients as previously described (Pollard et al., 1992; Seiwert et al., 1996). RNAs were heated to 60 °C and slowly cooled to 27 °C at a rate of 2 °C per minute. Ten microliters of an active glycerol fraction were then added. Reactions were incubated at 27 °C for 20 min. Conditions of the reactions were as follows: 20 mM HEPES, pH 7.9, 50 mM KCl, 10 mM MgOAc, 0.05 mM DTT, 1 mM EDTA, and 5 mM $CaCl_2$. Each reaction contained 30 Kcpm of 5′-end-labeled RNA (approximately 25 fmol). The amount of gRNA used in each reaction is specified in the figure legends.

ACKNOWLEDGMENTS

This work was supported by National Institutes of Health Grant AI34155 to D.K. Many thanks to Dr. Ron Patterson, Sandra Clement, Laura Bean, and Larissa Reifur for critical reading of the manuscript and helpful discussions.

Received February 1, 2001; returned for revision April 5, 2001; revised manuscript received September 18, 2001

REFERENCES

Bhat GJ, Koslowsky DJ, Feagin JE, Smiley BL, Stuart K. 1990. An extensively edited mitochondrial transcript in kinetoplastids encodes a protein homologous to ATPase subunit 6. *Cell 61*:885–894.

Blum B, Simpson L. 1990. Guide RNAs in kinetoplastid mitochondria have a nonencoded 3′ oligo(U) tail involved in recognition of the preedited region. *Cell 62*:391–397.

Burgess ML, Heidmann S, Stuart K. 1999. Kinetoplastid RNA editing does not require the terminal 3′ hydroxyl of guide RNA, but modifications to the guide RNA terminus can inhibit in vitro U insertion. *RNA 5*:883–892.

Burgin AB, Pace NR. 1990. Mapping the active site of ribonuclease P RNA using a substrate containing a photoaffinity agent. *EMBO J 9*:4111–4118.

Byrne EM, Connell GJ, Simpson L. 1996. Guide RNA-directed uridine insertion RNA editing in vitro. *EMBO J 15*:6758–6765.

Christiansen J, Egeberg J, Larsen N, Garrett RA. 1990. Analysis of rRNA structure: Experimental and theoretical considerations. In: Speding G, ed. *Ribosomes and protein synthesis: A practical approach.* New York: Oxford University Press. pp 229–252.

Corell RA, Read LK, Riley GR, Nellissery JK, Allen TE, Kable ML, Wachal MD, Seiwert SD, Myler PJ, Stuart KD. 1996. Complexes from *Trypanosoma brucei* that exhibit deletion editing and other editing-associated properties. *Mol Cell Biol 16*:1410–1418.

Cruz-Reyes J, Piller KJ, Rusché LN, Mukherjee M, Sollner-Webb B. 1998. Unexpected electrophoretic migration of RNA with different 3′ termini causes a RNA sizing ambiguity that can be resolved using nuclease P1-generated sequencing ladders. *Biochemistry 37*:6059–6064.

Cruz-Reyes J, Sollner-Webb B. 1996. Trypanosome U-deletional RNA editing involves guide RNA-directed endonuclease cleavage, terminal U exonuclease, and RNA ligase activities. *Proc Natl Acad Sci USA 93*:8901–8906.

Ehresmann C, Baudin F, Mougel M, Romby P, Ebel JP, Ehresmann B. 1987. Probing the structure of RNAs in solution. *Nucleic Acids Res 15*:9109–9128.

Estevez AM, Simpson L. 1999. Uridine insertion/deletion RNA editing in trypanosome mitochondria—A review. *Gene 240*:247–260.

Feagin JE, Abraham JM, Stuart K. 1988. Developmental aspects of uridine addition within mitochondrial transcripts of *Trypanosoma brucei*. *Mol Cell Biol 8*:1259–1265.

Feagin JE, Jasmer DP, Stuart K. 1987. Developmentally regulated addition of nucleotides within apocytochrome b transcripts in *Trypanosoma brucei*. *Cell 49*:337–345.

Göringer HU, Koslowsky DJ, Morales TH, Stuart K. 1994. The formation of mitochondrial ribonucleoprotein complexes involving guide RNA molecules in *Trypanosoma brucei*. *Proc Natl Acad Sci USA 91*:1776–1780.

Hajduk SL, Sabitini RS. 1998. Mitochondrial mRNA editing in kinetoplastid protozoa. In: Grosjean H, Benne R, eds. Modification and editing of RNA. Washington, DC: ASM Press. pp 377–393.

Hertzberg RP, Dervan PB. 1984. Cleavage of DNA with methidiumpropyl-EDTA-iron(II): Reaction conditions and product analyses. *Biochemistry 23*:3934–3945.

Igo RP, Palazzo SS, Burgess K, Panigrahi AK, Stuart K. 2000. Uridylate addition and RNA ligation contribute to the specificity of kinetoplastid insertion RNA editing. *Mol Cell Biol 20*:8447–8457.

Kable ML, Seiwert SD, Heidmann S, Stuart K. 1996. RNA editing: A mechanism for gRNA-specified uridylate insertion into precursor mRNA [see comments] [published erratum appears in *Science*, 1996, *274*:21]. *Science 273*:1189–1195.

Kapushoc ST, Simpson L. 1999. In vitro uridine insertion RNA editing mediated by *cis*-acting guide RNAs. *RNA 5*:656–669.

Kean JM, White SA, Draper DE. 1985. Detection of high-affinity intercalator sites in a ribosomal RNA fragment by the affinity cleavage intercalator methidiumpropyl-EDTA-iron(II). *Biochemistry 24*:5062–5070.

Koslowsky DJ, Kutas SM, Stuart K. 1996. Distinct differences in the requirements for ribonucleoprotein complex formation on differ-

entially regulated pre-edited mRNAs in *Trypanosoma brucei*. *Mol Biochem Parasitol 80*:1–14.
Kowalski D, Kroeker WD, Laskowski M. 1976. Mung bean nuclease I. Physical, chemical, and catalytic properties. *Biochemistry 15*: 4457–4463.
Leung SS, Koslowsky DJ. 1999. Mapping contacts between gRNA and mRNA in trypanosome RNA editing. *Nucleic Acids Res 27*: 778–787.
Leung SS, Koslowsky DJ. 2001. RNA editing in *Trypanosoma brucei*: Characterization of gRNA U-tail interactions with partially edited mRNA substrates. *Nucleic Acids Res 29*:703–709.
Mathews DH, Sabina J, Zuker M, Turner DH. 1999. Expanded sequence dependence of thermodynamic parameters improves prediction of RNA secondary structure. *J Mol Biol 288*:911–940.
Matzura O, Wennborg A. 1996. RNAdraw: An integrated program for RNA secondary structure calculation and analysis under 32-bit Microsoft Windows. *Comput Appl Biosci 12*:247–249.
Milligan JF, Groebe DR, Witherell GW, Uhlenbeck OC. 1987. Oligoribonucleotide synthesis using T7 RNA polymerase and synthetic DNA templates. *Nucleic Acids Res 15*:8783–8798.
Panigrahi AK, Gygi SP, Ernst NL, Igo RP, Palazzo SS, Schnaufer A, Weston DS, Carmean N, Salavati R, Aebersold R, Stuart KD. 2001. Association of two novel proteins, TbMP52 and TbMP48, with the *Trypanosoma brucei* RNA editing complex. *Mol Cell Biol 21*:380–389.
Piller KJ, Decker CJ, Rusché LN, Harris ME, Hajduk SL, Sollner-Webb B. 1995. Editing domains of *Trypanosoma brucei* mitochondrial RNAs identified by secondary structure. *Mol Cell Biol 15*:2916–2924.
Pollard VW, Harris ME, Hajduk SL. 1992. Native mRNA editing complexes from *Trypanosoma brucei* mitochondria. *EMBO J 11*:4429–4438.
Read LK, Göringer HU, Stuart K. 1994. Assembly of mitochondrial ribonucleoprotein complexes involves specific guide RNA (gRNA)-binding proteins and gRNA domains but does not require pre-edited mRNA. *Mol Cell Biol 14*:2629–2639.
Riley GR, Corell RA, Stuart K. 1994. Multiple guide RNAs for identical editing of *Trypanosoma brucei* apocytochrome b mRNA have an unusual minicircle location and are developmentally regulated. *J Biol Chem 269*:6101–6108.
Rusché LN, Cruz-Reyes J, Piller KJ, Sollner-Webb B. 1997. Purification of a functional enzymatic editing complex from *Trypanosoma brucei* mitochondria. *EMBO J 16*:4069–4081.
Schmid B, Riley GR, Stuart K, Göringer HU. 1995. The secondary structure of guide RNA molecules from *Trypanosoma brucei*. *Nucleic Acids Res 23*:3093–3102.
Schultz PG, Dervan PB. 1983. Sequence-specific double-strand cleavage of DNA by penta-N-methylpyrrolecarboxamide-EDTA X Fe(II). *Proc Natl Acad Sci USA 80*:6834–6837.
Seiwert SD, Heidmann S, Stuart K. 1996. Direct visualization of uridylate deletion in vitro suggests a mechanism for kinetoplastid RNA editing. *Cell 84*:831–841.
Stuart K, Allen TE, Heidmann S, Seiwert SD. 1997. RNA editing in kinetoplastid protozoa. *Microbiol Mol Biol Rev 61*:105–120.
Uchider T, Egami F. 1967. The specificity of ribonuclease T2. *J Biochem 61*:44–53.
Vary CP, Vournakis JN. 1984. RNA structure analysis using methidiumpropyl-EDTA.Fe(II): A base-pair-specific RNA structure probe. *Proc Natl Acad Sci USA 81*:6978–6982.
Wower J, Aymie M, Hixson SS, Zimmermann RA. 1989. Photochemical labeling of bovine pancreatic ribonuclease A with 8-azidoadenosine 3′,5′-bisphosphate. *Biochemistry 28*:1563–1567.